Symposium on Applied Aerodynamics and Design of Aerospace Vehicle (SAROD 2011)
November 16-18, 2011, Bangalore, India

CFD ANALYSIS TO INVESTIGATE THE EFFECT OF AXIAL SPACING IN A SINGLE STAGE TRANSONIC AXIAL FLOW COMPRESSOR

Hanoca P*, Shobhavathy M T**
Council of Scientific and Industrial Research-National Aerospace Laboratories, Bangalore, India

ABSTRACT

The axial spacing between the rotor and stator is an important parameter and has a strong influence on the performance of axial turbomachines. A study has been carried out to verify the effect of axial spacing on the performance of 1.35 pressure ratio single stage transonic compressor stage through CFD analysis using commercial code ANSYS FLUENT. Standard k-ε turbulence model with standard wall function is used for analysis. Reynolds Averaged Navier-Stokes equations are discretized with finite volume approximations using hybrid grids. First the analysis has been carried out for the baseline configuration of the compressor stage having an axial blade spacing of 75% of the rotor tip axial chord. The steady flow computations have been carried out for four speeds namely 43%, 60%, 80% and 90% of the compressor design speed and obtained the overall performance characteristics of the compressor stage. For validation, CFD values are compared with the experimental results. CFD results showed good agreement with the experiments and hence, the analysis has extended to four more axial spacing configurations such as 30%, 60%, 90% and 120% of the rotor tip axial chord. This study shows that for getting best operating conditions, the axial spacing for the referred compressor stage should lie in the range of 65 to 75% of rotor tip axial chord.

Key words: Axial compressor, Axial spacing, Overall performance characteristics, Operating range, Computational Fluid Dynamics.

NOMENCLATURE

P_0	Total Pressure (Pa)
P_s	Static Pressure (Pa)
M	Mach number
I	Turbulence intensity
D	Diameter (m)
D_t	Tip diameter
D_{IH}	Hub hydraulic diameter at inlet
D_{OH}	Hub hydraulic diameter at outlet
R	Radius (m)
Re	Reynolds number
c_{ax}	Rotor blade tip section axial chord (m)
d	Axial spacing (% of blade axial chord)
u	velocity (m/s)
Greek letters:	
γ	specific heat ratio
k	Turbulent Kinetic Energy(m^2s^{-2})
ν	kinematic viscosity (m^2/s)

* M. Tech Student
UBDT College of Engineering, Davangere-577004 (Karnataka)

** Scientist, Axial Flow Compressor Research Rig, Propulsion Division, CSIR-NAL, Bangalore.

1. INTRODUCTION

In the recent decades, the gas turbines have dominated air transportation by virtue of their high efficiency and reliability. An axial compressor is an important part of any efficient gas turbine. Axial flow compressors are the fluid pumping machinery where the fluid enters and exits axially to the rotor axis. The unique features like high mass flow rate for a small frontal area and high efficiency ratio with higher mass flow rate makes multistage axial flow compressors a perfect choice for gas turbines used in jet engines. The performance and reliability of a gas turbine heavily relies on its axial compressor module. Higher stability margin is paramount for successful operation of an axial compressor and also for its reliability. The efficiency and stability margin of an axial compressor is mainly defined by aero thermal design. Every axial flow compressor has a limit on its mass flow, at both higher and lower side for a specific speed called its operating range, within which it can operate successfully. The maximum mass flow rate is called choke limit. The peak efficiency point is normally referred as the design point. The minimum mass flow rate at which the compressor can run stably is called the stall point. At the stall point aerodynamic instabilities would be initiated. Beyond this point local flow re-circulation would be induced due to flow separation.

The present day research and developmental efforts in the area of axial flow compressors for aero-engine application are aimed at reducing the size and

weight and at improving its operating range without sacrificing efficiency. The reduction in weight is possible through (i) reduction in the number of stages, (ii) application of alternate light-weight material like Carbon Fiber Reinforced Plastics for blades and discs. By reducing the number of stages and diameter of the compressor, reduces the size of the compressor but leads to increased blade loading per stage, turbine matching problem and increased rotational speeds which are detrimental to the performance of the compressor. It is known that, the engine weight can also be reduced by decreasing the axial spacing between blade rows in the compressor. The smaller axial spacing makes a more compact engine, thereby making the aircraft configuration layout easier. It is known as well that, axial spacing is a very important parameter and it has a strong influence on the performance of the axial Turbomachines. Several experimental and numerical investigations have been performed in the past, studying the effects of axial spacing on compressor performance, but yielded mixed results. Smith L H, 1966[1], Mikolajczak, 1976[3], John J. Adamczyk, 1996[4] found closer axial spacing to be beneficial, while Hetherington and Moritz,1977[5] and Gorrell et al.,2002a[8] observed a decrease in efficiency at closer gaps. Earlier studies of blade-row interactions were focused on subsonic flows through gas turbine engines and only in recent years the studies have been examined in transonic flow conditions. The investigations performed by Zachcial and Nürnberger, 2003 [7] compared the performances of subsonic and transonic operating conditions. Their results showed that subsonic flows have opposite trends to that of the transonic flows. However, the findings of Zachcial and Nürnberger are contrary to the results of the investigation by Gorrell et al. No agreement on the influence of axial spacing between blade-rows for transonic simulations and experiments has been reached.

This paper describes the application of commercial 3-Dimensional Computational Fluid Dynamics(CFD) code ANSYS FLUENT to investigate the influence of axial spacing on a high speed single stage transonic axial flow research compressor at National Aerospace Laboratories. The first goal was to predict the overall performance map for the baseline configuration of the research compressor, which is having axial spacing of 75% of the rotor tip axial chord (c_{ax}) and compare with experimental data for validation. The second goal was the CFD analysis of compressor stage at various axial spacing (d) configurations such as 30%, 60%, 90% and 120% of c_{ax} to obtain the overall performance to find the best axial spacing in-terms of pressure ratio, isentropic efficiency and operating range of the compressor.

Main specification of axial flow compressor:

Type of compressor	: Single Stage Transonic Axial Flow
Corrected rotational speed	: 12930 rpm
Corrected mass flow rate	: 22 kg/s
Stage total pressure ratio	: 1.35
Stage adiabatic efficiency	: 89%
Rotor tip diameter	: 450 mm

The research compressor stage comprises a NACA transonic rotor having 21 blades and a subsonic stator having 18 blades. The axial blade spacing is 75% of c_{ax}[1]. The schematic of the research compressor stage is shown in Figure 1.

2. NUMERICAL ANALYSIS OF THE RESEARCH COMPRESSOR BASELINE CONFIGURATION

A steady state flow numerical analysis has been carried out using ANSYS FLUENT code for four speeds such as 43%, 60%, 80% and 90% of the research compressor design speed and obtained the overall performance characteristics of the compressor stage. These values are compared with the experimental results for validating the CFD code.

a. Solid Modelling of the Flow Domain

The solid modeling of the rotor and stator were made with the help of CAD tools CATIA as shown in Figure 2. A single passage with one rotor blade and one stator blade instead of 360° model was considered for flow analysis to reduce the grid size. The flow field domain for the baseline configuration was divided into six sub volumes to have a choice of hybrid grid generation and fixing up the boundary conditions appropriately. The sub volumes are volume-1, rotor-volume, volume-2, volume-3, stator-volume and volume-4 as shown in the Figure 3.

2.2 Grid Generation

The grid was generated for the flow domain using “Geometry and Mesh Building Intelligent Toolkit”(GAMBIT). Size function was used for resolving boundary layers. Because of the complexity of the geometry, the flow domain was meshed with hybrid grids. The volume 1, volume 2, volume 3 and volume 4 as labeled in the Figure 3 having simple geometry and were meshed with structured grids. The rotor volume and the stator volume are having complicated geometry and were meshed with unstructured grids as shown in the Figure 4. The boundary types were defined appropriately such as

pressure at inlet and outlet, interface, periodic and walls as shown in Figure 5.

2.3 Flow Analysis

a) Numerical algorithm

3-D steady Navier-Stoke equations were solved using segregated pressure based implicit solver by ANSYS FLUENT. Standard k–ε turbulence viscosity model with SIMPLE pressure-velocity coupling and First-Order Upwind discretization scheme was used for the analysis.

b) Boundary conditions

A no-slip condition was specified for the flow at the wall boundaries of the blade, hub and casing for both rotor and stator fluid. A periodic condition was applied to the rotor and stator fluid. A static pressure at exit with radial equilibrium condition was specified as shown in the Figure 5. The interface between the rotor and the stator plane was set to a mixing plane, in which the flow data at the mixing plane interface are averaged in the circumferential direction both at rotor outlet and the stator inlet boundaries and are updated at each iteration.

c) Solution methodology

To obtain the operating range of the compressor for a particular speed, the solutions for different exit pressures (back pressure) were obtained till the compressor gets in to stall at that specified speed. Towards the stall condition of the compressor, the exit static pressure was required to be increased in small steps to get converged solution. Convergence of solution was monitored through the use of residuals of the system of algebraic equations. The residuals were set to stop the solution once they dropped below a certain value. In this analysis, energy residual criterion is specified to 1×10^{-8} to get more accurate solution. Figure 6 shows the typical convergence history of mass flow rate on stator outlet and Figure 7 shows the typical variation of residuals of various parameters like mass flow, velocity components and energy against the number of iterations carried out. In these figures, y-axis represents the variable parameters and x-axis represent the number of iterations.

2.4 Grid Independence Test

In order to ensure that the solution is not affected by the size of the grid, a grid independence study was carried out by taking three different grid configurations and observing their convergence behaviour at 43% of design speed of the compressor. The overall mesh size and worst element skewness for the three grid configurations are shown in Table-I. Case–A, Case-B, and Case-C are the three grid configurations. All these cases were compared with baseline experimental results. Case-A was the coarse grid with 567020 mesh elements, which resulted in early stall. The Case-B had 1066694 elements, which showed a realistic behaviour and solution was close to experimental stall point. Case–C had 1172597 elements and showed no significant variation in the results as compared to that of Case-B and consequently, Case-B was chosen for all further analysis. The performance characteristics obtained by these three different grid configurations were compared with the experimental results as in shown Figure 8.

2.5 Validation of the Predicted Values

The predicted overall performance values were validated by comparing with the experimental results of the test compressor. Figure 9 shows the variation of total pressure ratio and adiabatic efficiency against the corrected mass flow rate for the predicted and experimental results. From this figure, it can be observed that there is an appreciable agreement between the experimental results and the CFD values at different off-design conditions of the compressor.

2.6 Flow Features of the Baseline Configuration

The detailed flow features of the baseline configuration, at 90% of design speed will be discussed below with reference to the Mach number contour plots, and the axial velocity contour plots at different flow conditions. In this discussion, different flow conditions will be identified by points A1, A2 and A3 as labeled in the performance characteristics shown in Figure 9. The point labeled as A1 corresponds to choked condition, A2 to maximum efficiency condition and A3 to near stall condition. Figure 10.1 shows the relative Mach number contour plot on a tangential plane near casing for case A1. From this figure, it can be seen that, the strong shock in the rotor passage near trailing edge on suction surface is extending little below the mid-chord region on pressure surface. The flow in the stator is smooth. Figure 10.2 shows the Mach number contour plot near the casing for case A2 (max. efficiency condition). It shows that, the shock position is slightly shifted towards the leading edge as compared to case A1. The flow in the stator is smooth. For case A3, the result shows that, the shock position is further shifted towards the leading edge of the rotor and the flow in the stator is smooth. In these figures it can be observed the presence of low energy fluid at the

trailing edge of the rotor in all flow conditions. This is due to the tip leakage flow at the rotor tip clearance. This can be visualized clearly from the velocity vector, which gives a 3-dimensional feel of the flow field at the rotor tip clearance. Figure 11 shows the typical velocity vector plot at the rotor casing at 90% of design speed and at maximum efficiency condition.

Figure 12 shows the axial velocity contour plots taken at a plane exit to the rotor at 90% of design speed. Figure 12.1, 12.2 and 12.3 are the velocity contours for the case A1, A2 and A3 respectively. These figures clearly show the flow deceleration and hence, building up of pressure at the rotor exit while the compressor flow condition shifts from choking to the stalling condition.

3. NUMERICAL ANALYSIS OF THE COMPRESSOR STAGE AT FOUR DIFFERENT AXIAL GAPS

The four configurations of the compressor stage at different axial spacings such as 30%, 60%, 90% and 120% of the c_{ax} were generated and are shown in the Figure 13. CFD analysis was carried out for all the configurations similar to that of the baseline configuration.

4. RESULTS AND DISCUSSION

The overall performance characteristics of the compressor at four different axial spacing were obtained at different off-design rotational speeds of the rotor and compared with the baseline configuration. Figure 14 shows the comparative performance maps for 30% of c_{ax} configuration and baseline case. It showed that, at 30% of c_{ax} case, the compressor efficiency, pressure ratio as well as the operating range of the compressor reduced compared to that of the baseline configuration. The observed loss in efficiency, pressure ratio and operating range were 10%, 3.32% and 7.3% respectively at 80% design speed. The computing time taken for 30% of c_{ax} case was four times higher to that of baseline configuration.

Figure 15 shows the comparative performance maps for 60% of c_{ax} and baseline configurations. It was observed that, there was a gain in efficiency of 3.5% in all speeds of the rotor at 60% of c_{ax} case. The pressure ratio curves at lower operating speeds have traced over the baseline configuration, but at 90% design speed, there was a gain in pressure ratio of 1.34% with a loss in operating range of 7.6% compared to that of baseline configuration. The computing time was double the baseline configuration.

Figure 16 shows the comparative performance maps for 90% of c_{ax} and baseline configurations. At 90% of c_{ax} case , there were negligible losses both in efficiency and pressure ratio which were in the order of 0.1 to 0.01% . The operating range was reduced in all speeds. The maximum drop in operating range was 6.8% at 90% design speed. The computing time taken was double to that of baseline configuration.

Figure 17 shows the comparative performance maps for 120% and baseline configurations. At 120% of c_{ax}, it was observed that, the pressure ratio curves were traced over the baseline configuration but with a reduction in operating range in all speeds. The maximum reduction in operating range observed was 6.4% at 90% design speed. It was also noticed that there is a reduction in efficiency of 1.09% as compared to that of baseline configuration. The computing time was approximately 1.5 times greater than that of baseline configuration.

Figure 18 shows the consolidated comparative plot for the total pressure, efficiency and the mass flow rate at the near stall condition at 80% design speed, as compared to the design point parameters. Through this study it has been clearly brought out that the best axial spacing for the referred compressor stage is 65 to 75% of axial chord of the rotor at tip section.

The flow features of the compressor at different axial gaps were studied with the help of Mach number profiles at rotor exit and static temperature contours at the rotor casing. The Mach number contours were taken at a plane; exit to the rotor and 5mm a head to the stator at 80% design speed and at maximum efficiency condition for all the axial spacing configurations. These contours are indicated as (i), (ii), (iii), (iv) and (v) in the Figure 19 for the corresponding axial gaps of 30, 60, 75, 90 and 120%. These contours show that, the rotor wake becomes longer and wider as the axial gap is increased. When the rotor wake becomes too longer, compared to the axial chord of the rotor as in the case of 120% of axial spacing, the efficiency of the compressor was decreased. This may be due to a less wake recovery effects in the longer rotor wakes as mentioned in the reference [2], [4].

Figure 20 shows the comparative static temperature contours taken at rotor casing for different axial gaps at 80% design speed and at near stall flow conditions. These contours show that, the static temperature raised is highest for the case of 30% axial spacing configuration as compared to all

other cases. This may be due to the severe interaction between the rotor wakes and stator blades at lesser axial spacing as stated in the references [8-9]. These references have pointed out that, in a transonic compressor, with lesser axial spacing, the wakes of the rotor are sliced by the downstream stator and reflects a strong pressure waves from the stator blade surfaces, which travel upstream, striking the rotor blade surface. These processes increase the temperature and entropy of the system, which yield to decrease in compressor efficiency.

5. CONCLUSION

A steady state CFD analysis has been carried out on a single stage transonic axial flow compressor of 1.35 pressure ratio to obtain the overall performance of the compressor at various off-design conditions using commercial code ANSYS FLUENT. The CFD values are compared with the experimental results available at Axial Flow Compressor Research Rig, National Aerospace Laboratories (NAL), Bangalore to validate the CFD code. The predicted values had good agreement with the experimental data.

CFD analysis was extended to four different configurations of the compressor with different axial spacing, to verify the influence of axial spacing on the performance of the referred compressor stage.

Through this study, it has been clearly brought out that, the best axial spacing for the referred compressor stage is 65% to 75% of the rotor tip axial chord.

ACKNOWLEDGMENT

The authors would like to thank Dr A R Upadhya, Director, CSIR-NAL, Bangalore for his kind permission to carry out this study at NAL Thanks are due to Head, Propulsion Division for supporting to take up this research work at the Divisional Facility. The author's also like to thank the team members of the Axial Flow Compressor Rig, for their cooperation during the course of study.

REFERENCES

[1] K.Mohan, Q.H.Nagpurwala, H.Girigoswamy, S.A.Guruprasad:"High speed Axial Flow Compressor Research Facility", NAL-TM-PR-UN-0-(103), 103/1/1981.

[2] Smith, L. H., Jr.: ''Wake Dispersion in Turbomachines,'' J. Basic Eng., pp. 688–690, 1966.

[3] Mikolajczal, A. A., 1976:"Practical Importance of Unsteady Flow, Unsteady Flow Phenomena in Turbomachinery", AGARD CP. 177, and North Atlantic Treaty Organization.

[4] Adamczyk, J.J. et al: "Wake Recovery Performance Benefit in a High-Speed Axial Compressor" Journal of Turbomachinery 2002 by ASME APRIL 2002, Vol. 124

[5] Hetherington, R. and Moritz, R. R.: "The Influence of Unsteady Flow Phenomena on the Design and Operation of Aero Engines". Unsteady Flow Phenomena in Turbomachinery, AGARD CP. 177, and North Atlantic Treaty Organization.

[6] R.Parker. Journal, "Relation between Blade Row Spacing and Potential Flow Interaction Effects in Turbomachines", lnstn Mech Engrs 1969-70 Vol 184 Pt 3G.

[7] Zachcial, A. and Nürnberger, D:". A Numerical Study on the Influence of Vane-Blade Spacing on a Compressor Stage at Sub- and Transonic Operating Conditions", ASME Paper No. GT2003-38020, ASME Turbo Expo 2003, Atlanta, Georgia.

[8] Gorrell, S. E., Okiishi, T. H., and Copenhaver, W.W., 2002a: "Stator-Rotor Interactions in a Transonic Compressor Part 1. Effect of Blade-Row Spacing on Performance". ASME Paper No. GT-2002-30494, AMSE Turbo Expo 2002, Amsterdam, the Netherlands.

[9] Gorrell, S. E., Okiishi, T. H., and Copenhaver, W. W., 2002b: "Stator-Rotor Interactions in a Transonic Compressor Part 2. Description of a Loss Producing Mechanism". ASME Paper No. GT-2002-30495, AMSE Turbo Expo 2002, Amsterdam, the Netherlands.

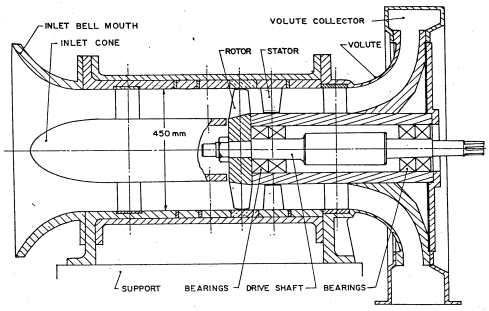

Figure 1. Schematic of the research compressor

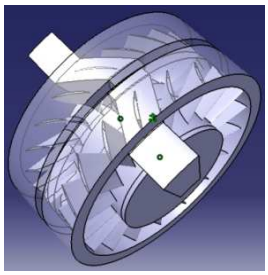

Figure 2. 3D modeling of the flow domain in a compressor stage

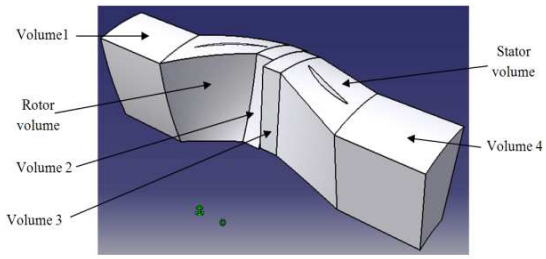

Figure 3. Flow field domain of baseline configuration

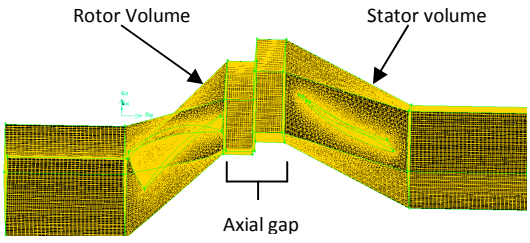

Figure 4. Meshed flow domain

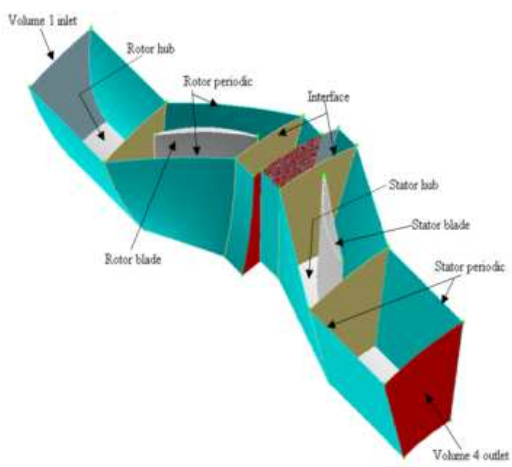

Figure 5. Boundary conditions applied to the flow Domain

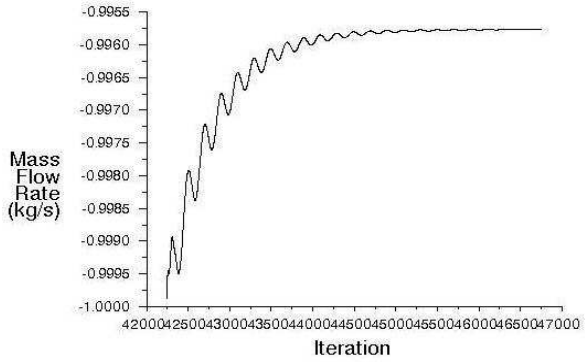

Figure 6. Typical convergence history of mass flow rate on stator outlet

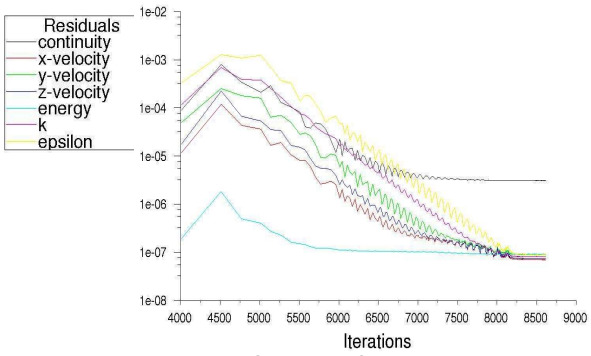

Figure 7. Residuals of various flow parameters

Table I. Grid parameter for case A case B and case C

Case	Over all mesh size	Worst element skewness
Coarse mesh (A)	567020	0.79
Medium (B)	1066694	0.80
Fine mesh (C)	1172597	0.80

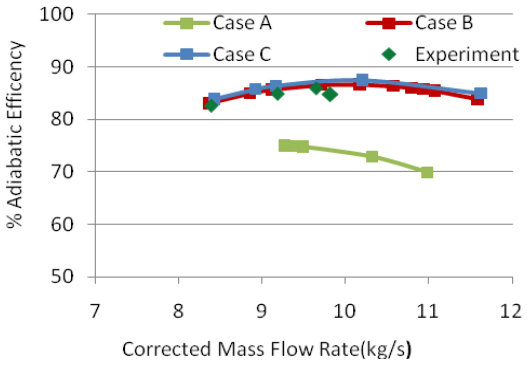

Figure 8. Performance characteristic curves at 43% of design speed for Case A, B , C and experimental data

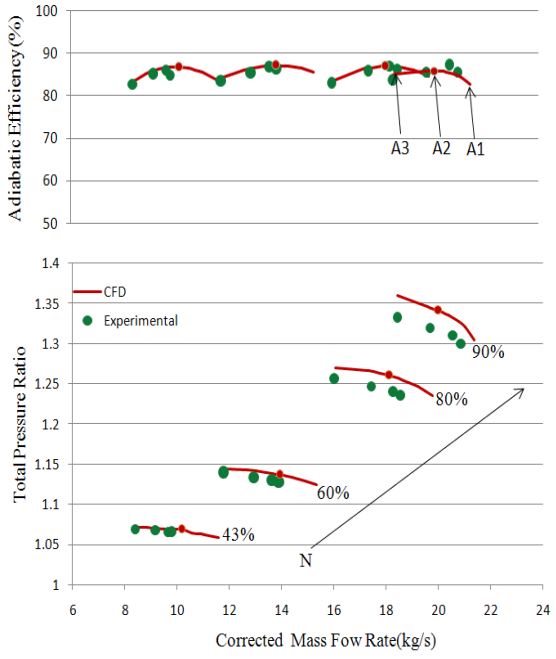

Figure 9. Predicted and experimental performance map of the compressor at baseline configuration

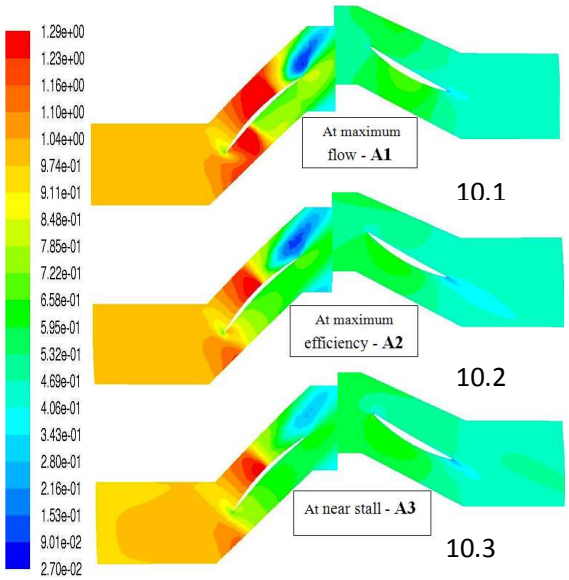

Figure 10. Mach number contours at choked flow, maximum efficiency and near stall conditions at 90% design speed of the compressor.

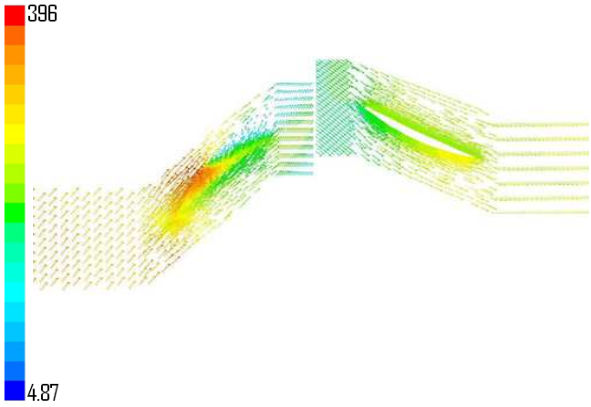

Figure 11. Velocity vectors at rotor casing at 90% design speed and at maximum efficiency flow condition.

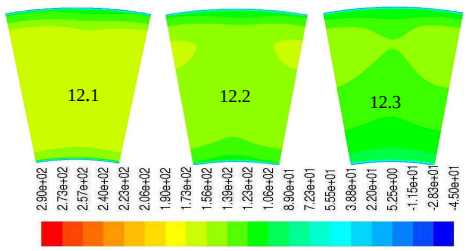

Figure 12. Axial velocity contour at rotor exit at 90% design speed for (i) choked flow (ii) max

efficiency and at (iii) near stall flow conditions of the baseline configuration

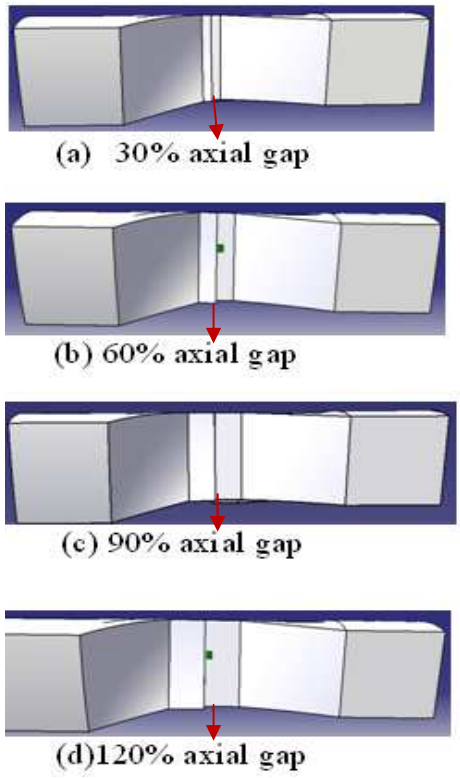

Figure 13. Compressor stage configuration at different axial gap between rotor and stator.

condition.

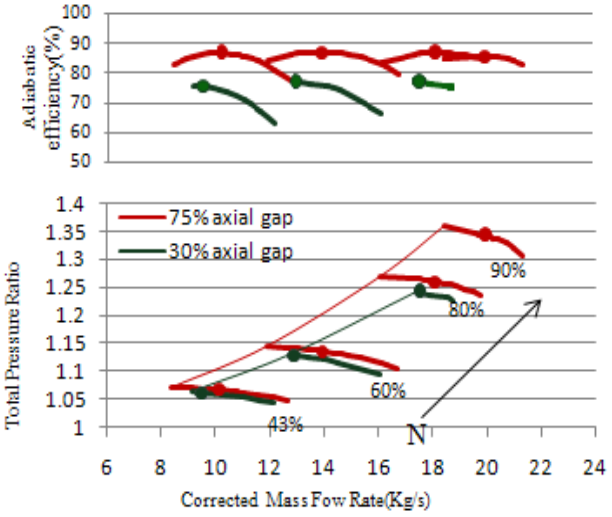

Figure 14. Comparative performance maps at 30% and 75% axial chord

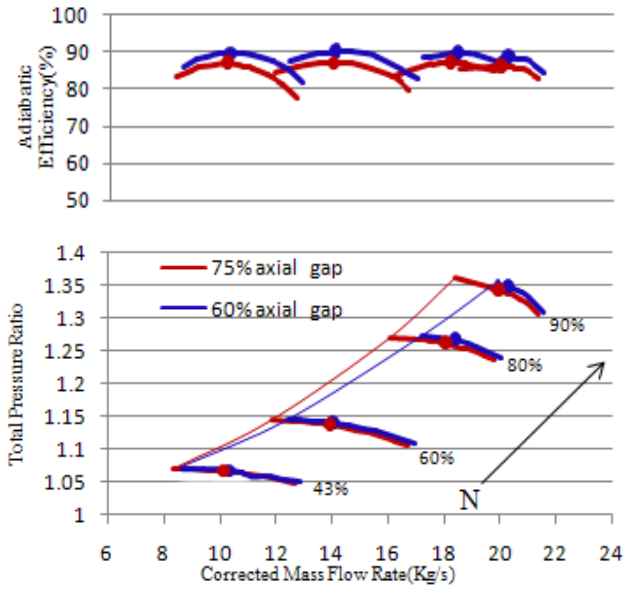

Figure 15. Comparative performance maps at 60% and 75% axial chord

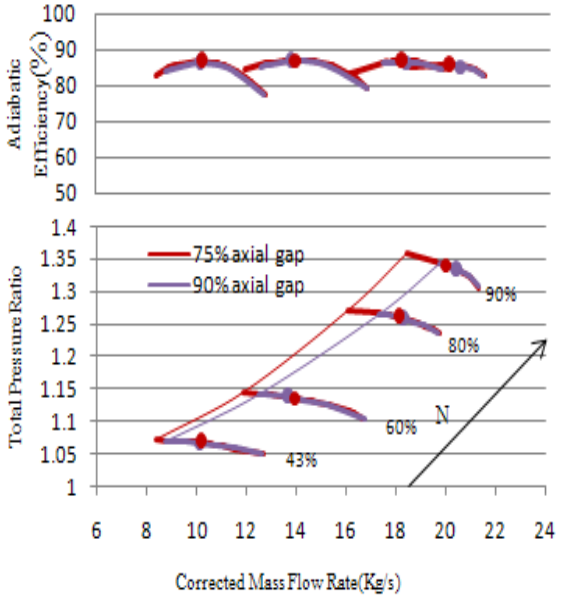

Figure 16. Comparative performance maps at 90% and 75% axial chord

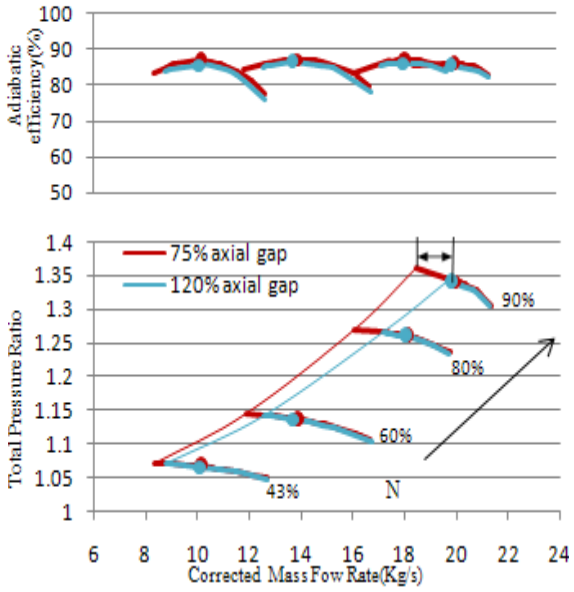

Figure 17. Comparative performance maps at 120% and 75% axial chord

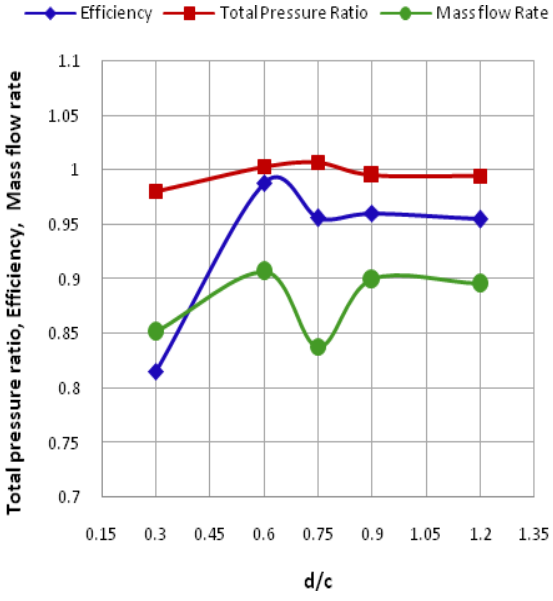

Figure 18. Comparative plots for the total pressure ratio, efficiency and mass flow rate at 80% design speed for 30, 60, 75, 90 and 120% of axial gap at near stall flow

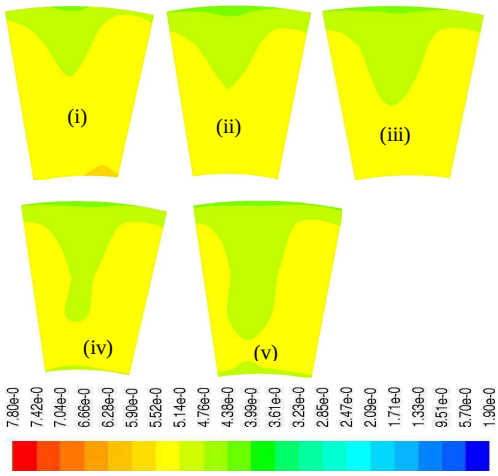

Figure 19. Span wise Mach number contours at different axial spacing configurations taken at a plane exit to rotor at 80% design speed and at maximum efficiency flow condition.

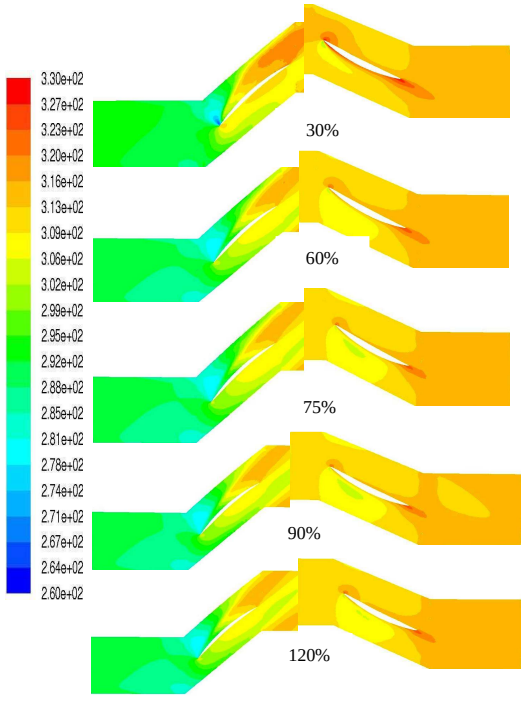

Figure 20. Static temperature contours at different axial spacing at 80% design speed and at near stall flow conditions.